# Inhibition of apoptosis by BCL2 prevents leukemic transformation of a murine myelodysplastic syndrome

Christopher I Slape[1,2], Jesslyn Saw[1,2], Jeremy B M Jowett[3], Peter D Aplan[4], Andreas Strasser[5,6], Stephen M Jane[1,2,7] and David J Curtis[1,2,7]

[1]Bone Marrow Research Laboratories, Royal Melbourne Hospital, Parkville, VIC, Australia; [2]Division of Blood Cancers, Australian Centre for Blood Diseases, Central Clinical School, Monash University, Melbourne, VIC, Australia; [3]Genomics and Systems Biology, Baker IDI Heart and Diabetes Institute, Melbourne, VIC, Australia; [4]Genetics Branch, Center for Cancer Research, National Cancer Institute, National Institutes of Health, Bethesda, MD, USA; [5]The Walter and Eliza Hall Institute of Medical Research, Parkville, VIC, Australia; [6]Department of Medical Biology, The University of Melbourne, Melbourne, VIC, Australia; [7]Department of Clinical Hematology, Alfred Hospital, Melbourne, VIC, Australia

Short title: BCL2 prevents transformation of MDS

Corresponding author: Christopher Slape

E-mail: christopher.slape@monash.edu

Postal address: Monash University, Central Clinical School, The Alfred Centre, 99 Commercial Rd, Melbourne 3004, Australia

Phone: +61 3 9903 0619 Fax: +61 3 99032 4293

Word Count: Abstract: 200 Text: 3366

Figure Count: 7

Reference Count: 39

Scientific Category: Myeloid Neoplasia

## Abstract

Programmed cell death or apoptosis is a prominent feature of low risk myelodysplastic syndromes (MDS), although the underlying mechanism remains controversial. High risk MDS have less apoptosis associated with increased expression of the pro-survival BCL2-related proteins. To address the mechanism and pathogenic role of apoptosis and BCL2 expression in MDS, we used a mouse model resembling human MDS, in which the fusion protein NUP98-HOXD13 (NHD13) of the chromosomal translocation t(2;11)(q31;p15) is expressed in hematopoietic cells. Hematopoietic stem and progenitor cells from three-month old mice had increased rates of apoptosis associated with increased cell cycling and DNA damage. Gene expression profiling of these MDS progenitors revealed a specific reduction in *Bcl2*. Restoration of *Bcl2* expression by a *BCL2* transgene blocked apoptosis of the MDS progenitors, which corrected the macrocytic anemia. Blocking apoptosis also restored cell cycle quiescence and reduced DNA damage in the MDS progenitors. We expected that preventing apoptosis would accelerate malignant transformation to AML. However, contrary to expectations, preventing apoptosis of pre-malignant cells abrogated transformation to AML. In contrast to the current dogma that overcoming apoptosis is an important step towards cancer, this work demonstrates that gaining a survival advantage of pre-malignant cells may delay or prevent leukemic progression.

## Introduction

Myelodysplastic syndromes (MDS) are a heterogeneous group of malignant clonal disorders of hematopoietic stem cells (HSC), characterized by reduced peripheral blood cell counts (cytopenias) with dysplasia in one or more cell lineages and increased risk of progression to acute myeloid leukemia (AML)[1]. Apoptosis is a prominent feature of the World Health Organization (WHO) low-intermediate risk subgroups of MDS, although whether apoptosis is directly responsible for the cytopenias remains unproven. Mammals possess two major apoptotic pathways, the death receptor pathway and the BCL2-regulated (also called stress, mitochondrial or intrinsic) pathway[2]. Increased apoptosis in MDS has been attributed to activation of the death receptor pathway[3], although recent studies of a mouse model of the WHO del(5q) subtype have implicated the BCL2-regulated pathway through activation of TP53[4].

As in other cancers[5,6], oncogene-induced apoptosis in MDS may function as a protective mechanism by reducing the pool of pre-malignant cells that can acquire additional genetic or epigenetic changes required for progression to AML. As such, overcoming apoptosis may be an important mechanism of malignant transformation to AML[6]. Consistent with this notion, more aggressive, high risk subgroups of MDS have an increased expression of anti-apoptotic BCL2-related proteins relative to pro-apoptotic BH3-only proteins[7].

One of the major hurdles of studying MDS is the genetic and cellular heterogeneity of human MDS and the inability to grow primary samples *in vitro* or in immune-deficient mouse strains. To this end, we have generated a transgenic mouse model of MDS by hematopoietic-expression of the fusion gene *Nup98-HoxD13* (*NHD13*) of the t(2;11)(q31;p15) chromosomal translocation[8]. The *NHD13* model recapitulates many of the features of human MDS, with an early pre-leukemic phase of cytopenias and increased apoptosis in the bone marrow followed by

the development of AML harboring mutations in genes such as *N-Ras*[9]. Here, we have used this MDS model to investigate the role of apoptosis in cytopenias and leukemic transformation.

## Materials and Methods

**Mice.** The *NHD13* mice have been described previously[8]. *Tnf*$^{-/-}$ mice were kindly provided by Dr B Saunders, The University of Sydney[10]. The *Fas*$^{gld/gld}$ mice were obtained from the Walter and Eliza Hall Institute for Medical Research, Melbourne[11]. The *BCL2* transgenic mice were kindly provided by Dr P Bouillet and Professor J Adams, The Walter and Eliza Hall Institute for Medical Research[12]. All mice were maintained on a C57BL/6J background. All animal experiments were approved by the Animal Ethics Committee, University of Melbourne.

**FACS Analysis.** BM samples were flushed from femora and tibiae into PBS containing 2% fetal bovine serum (FBS). Antibodies and other reagents for staining were obtained from BD Pharmingen (San Diego, CA): Annexin-V (51-6874) and Ki67 (B56) as fluorescein isothiocyanate (FITC) conjugates; c-KIT (Ack45), SCA (E13-161.7), CD8a (53-6.7) and mouse BCL2 (3F11) as phycoerythrin (PE) conjugates; CD4 (RM4-5), c-KIT (2B8) as allo-phycocyanin (APC) conjugates; SCA-1 (D7) as a tandem PE and Cy7 conjugate; γ-H2AX (20E3) as an Alexa-647 conjugate; and biotinylated Mac-1 (M1/70), Gr-1 (RB6-8C5), Ter-119, B220 (RA3-6B2) and CD3 (145-2C11). Second-stage reagents were either Streptavidin (SAv) APC, Sav Peridinin Chlorophyll Protein Complex (PerCP) or SAv APC-Cy7. Cellular DNA content was determined by staining with 4',6-diamidino-2-phenylindole (DAPI). Cell viability was measured by exclusion of propidium iodide (PI; Sigma, St Louis, CA). Caspase-3 activity levels were determined using the Vybrant assay kit (Molecular Probes; 35118). For cell permeabilization we used the BD Cytofix/cytoperm kit was according to the manufacturer's instructions. FACS analysis was performed using a FACSCalibur or LSR-II instrument (BD Biosciences). Cell sorting was performed using a FACSAria instrument (BD Biosciences).

**Hematopoietic Progenitor Assays.** BM cells were seeded at a density of 5 x $10^4$ cells per 35 mm dish in semi-solid agar for GM colony growth. Cultures were incubated at 37$^o$C in 10% $CO_2$ for 7 days, stained with acetyl-cholinesterase and counted. For BFU-E analysis, BM cells were seeded at 1X$10^5$ cells per 35 mm dish in methyl-cellulose (Methocel, Fluka Biochemical). Cultures were incubated in 5% $CO_2$ for 7 days, stained with diamino-benzidine and counted. All progenitor assays were performed in triplicate. TNF was dissolved in 2% FBS and added to cultures at the indicated concentrations. Micrographs were obtained on a Nikon Optiphot-2 using a 100x objective lens and a Zeiss Axiocam MRc5.

**Western Blotting.** FACS-sorted LK cells were derived from three mice of the appropriate genotype. Freshly isolated thymocytes were cultured in DMEM + 10% FBS in the presence or absence of FASL for 3 h. All cells were lysed in buffer containing 10 mM N-2-hydroxyethylpiperazine-N-2-ethanesulfonic acid, 250 mM Nonidet P-40, 5 mM ethylene-diaminetetraacetic acid and complete protease inhibitors (Roche). Proteins in cell lysates were separated by SDS-PAGE and transferred onto nitrocellulose membranes. Immunoblotting was performed with antibodies against caspase-8 (Cell Signaling; #9508) or b-actin (loading control; Santa Cruz; #1616) as per the manufacturer's instructions. Immunoblots were developed using an ECL kit with the secondary antibodies therein (GE Healthcare).

**Blood Cell Counts.** Blood samples were collected into EDTA-coated tubes and full blood counts were determined on an Advia 120 Automated Hematology Analyzer.

**Gene Expression Analysis.** Microarray analyses were performed using the Illumina iScan microarray platform (San Diego, CA). Briefly, total RNA was isolated from FACS-sorted LK cells from the pooled BM from three mice of each genotype by using the Trizol method and reverse transcribed using a T7-promoter-oligo(dT) primer. An *in vitro* transcription reaction with biotin labeled nucleotides (Ambion labeling protocol) was then performed, and the labeled cRNA samples were hybridized to the Illumina Mouse WG-6 v2.0 beadchip (45,281 transcripts), washed and scanned on the Illumina iScan. The resulting image files were analyzed using Illumina Beadstudio software to generate quantitative expression scores with mean standard deviation and statistical evaluation of detection reliability averaged across the 30-50 built-in technical replicates for each transcript. Differences in gene expression levels between *NHD13* mice and WT mice were determined by using three replicates from each group. The data analysis software package GeneSpring v11.5.1 was used to detect fold-change differences of >2 with a statistical significance of $p<0.05$ using the Student t-test on Log transformed data.

**Quantitative RT-PCR.** Total RNA was prepared from FACS-sorted LK cells by using the Trizol (Invitrogen, Carlsbad, CA) reagent according to the manufacturer's instructions. cDNA was transcribed from 1 mg of RNA using the Roche Transcriptor kit according to the manufacturer's instructions. Expression of *Cdkn1a* mRNA was quantified using the primer pair: sense 5'-ggtgggcccggaacatct-3', anti-sense 5'-gggccctaccgtcctactaat-3'. Expression of *BCL2* mRNA was quantified using the primer pair: sense 5'-gtacctgaaccggcatctg-3', anti-sense 5'-ggggccatatagttccacaa-3'. Expression of *Hoxc6* mRNA was quantified using the primer pair: sense 5'-cgaatgaattcgcacagtgg-3', anti-sense 5'-cggttctggaaccagattttg-3'. Expression of *Hoxb7* mRNA was quantified using the primer pair: sense 5'-ccctttgagcagaacctctcc-3', anti-sense 5'-Gtctggtagcgcgtgtaggtc-3'. Expression of *Hoxa9* mRNA was quantified using the primer pair:

sense 5'-aaacaatgccgagaatgagagcgg-3', anti-sense 5'-ttccgagtggagcgagcatgtagc-3'. Expression of *Pbx3* mRNA was quantified using the primer pair: sense 5'-ccaaattgacccagatcagac-3', anti-sense 5'-actgcttcacacgtgctttg-3'. Expression of all mRNA was normalized to expression of *b-actin*, which was quantified using the primer pair: sense 5'-gtacctgaaccggcatctg-3', anti-sense 5'-ggggccatatagttccacaa-3'. PCR reactions using the Promega GoTaq mastermix were performed on a LightCycler480 (Roche). PCR cycling conditions included an initial denaturation (95$^{o}$C 60 sec) followed by 95$^{o}$C 10 sec, 55$^{o}$C 10 sec and 72$^{o}$C 30 sec. Data were analyzed using the Roche LightCycler 480 software.

**Statistics.** Student's t test was used to determine significance of data, with the exception of animal survival studies for which we used the Mantel-Cox log rank test. All error bars represent the standard error of the mean (SEM).

## Results

**Increased apoptosis and proliferation of pre-malignant progenitor cells.** To characterize the apoptotic phenotype in early MDS, we analyzed *NHD13* mice at 3 months of age, when the animals displayed macrocytic anemia (reduced hematocrit and elevated red cell mean cell volume; MCV) and thrombocytopenia despite normal neutrophil counts (Fig. 1*A*). Lineage$^-$, c-Kit$^+$, Sca-1$^+$ (LKS) cells, a BM fraction enriched for HSC and multi-potent progenitor cells (HSPC), had increased apoptosis, as demonstrated by increased Annexin-V expression and caspase-3 activation (Fig. 1*B*). Increased apoptosis was also observed in the Lineage$^-$, Sca-1$^-$, c-Kit$^+$ (LK) myelo-erythroid progenitor cell fraction (Fig. S1). Staining of fixed LKS with the proliferation antigen Ki67 and the DNA fluorescent stain DAPI demonstrated reduced quiescence ($G_0$) of NHD13 stem and progenitor cells (Fig. 1*C*). Despite increased cell proliferation, total numbers of LKS cells were reduced four-fold, due to loss of the more mature Flk2$^+$ multi-potent progenitor cell fraction (Fig. 1*D*). Similar to human MDS[13], myeloid and erythroid progenitor cells displayed very poor *in vitro* growth with reduced numbers and size of colonies containing prominent numbers of dying cells (Fig. 1*E* and 1*F*). Overall, these analyses of *NHD13* hematopoietic progenitors revealed a picture typical of low-risk human MDS with increased cell proliferation and apoptosis[14].

**Apoptosis is not due to activation of the death receptor pathway.** Excessive apoptosis in MDS has been attributed to activation of the death receptor pathway within an abnormal bone marrow microenvironment[15]. To assess the role of the death receptor pathway in the apoptosis of *NHD13* hematopoiesis, we crossed *NHD13* mice with mice deficient in tumor necrosis factor ($Tnf^{-/-}$)[10] or Fas ligand ($Fasl^{gld/gld}$)[11]. The extent of apoptosis in BM from *NHD13*/$Tnf^{-/-}$ and

*NHD13*/*Fasl*$^{gld/gld}$ mice was comparable to that of control *NHD13* mice, with no decrease in the proportion of Annexin-V$^{+}$ LKS cells or rescue of the *in vitro* progenitor growth defects (Fig. 2*A-C*). Peripheral blood counts were also similarly affected by the *NHD13* transgene regardless of background (Fig. S2). To exclude activation of the death receptor pathway by other ligands, we examined for the presence of cleaved (activated) caspase-8, an essential component of this pathway[16]. Western blot analysis of LK cells from *NHD13* and wild-type littermate control mice did not reveal detectable levels of the activated form of caspase-8 (Fig. 2*D*). Wild-type thymocytes with or without Fas ligand (Fasl) served as controls, with a marked increase in cleaved caspase-8 seen with Fasl. These results suggest that activation of the death receptor pathway was unlikely to be an important mechanism of apoptosis in *NHD13* hematopoiesis.

**BCL2 prevents apoptosis and restores blood counts.** We compared the gene expression profile of LK cells isolated from three-month-old *NHD13* and wild-type mice to identify factors that might explain the increased apoptosis in *NHD13* hematopoiesis (Table S1). The most dramatic changes were increased expression of a number of homeobox genes (*Hoxc6*, *Hoxb7*, *Hoxa9* and *Pbx3*), many of which have been implicated in MDS and AML[17]. Analysis of genes regulating apoptosis revealed no abnormal expression of components of the death receptor pathway, consistent with our earlier findings (Fig. 2). The major apoptosis-related abnormality was a 3.6-fold reduction in *Bcl2* (Table S1). Q-RT-PCR confirmed reduced expression of *Bcl2* in LK cells (Fig 3A). Reduced expression of BCL2 protein in *NHD13* LK cells was confirmed by flow cytometry (Fig. 3B). Expression analysis of *BCL2*-related genes using a published array dataset of CD34$^{+}$ purified MDS bone marrow cells[18] revealed a significant reduction in *BCL2* in the del(5q) subset (Figure S3), where apoptosis has been linked to activation of the intrinsic pathway[4]. Increased expression of the pro-apoptotic genes *BID* and *PUMA* and the anti-apoptotic gene

*BCL-X* were also observed in the del5q subset but these changes were less marked and were not reflected in the *NHD13* progenitors.

The relative expression of the anti-apoptotic BCL2-related proteins is increased in higher risk human MDS[19]. Similarly, *Bcl2* expression was higher in AML cells arising in *NHD13* mice (Fig 3A). Therefore, the *NHD13* mouse model of MDS parallels the temporal changes in BCL2-related proteins seen in human MDS.

To evaluate the impact of reduced expression of BCL2 in early MDS, *NHD13* mice were crossed with *BCL2* transgenic mice, which express human *BCL2* in all hematopoietic cells[12]. Using Q-RT-PCR primers that amplify both mouse and human *BCL2* mRNA, we found that levels of *BCL2* in LK cells from *NHD13*/*BCL2* mice were increased 10-fold compared to wild-type LK cells (Fig. S4). Enforced *BCL2* expression inhibited apoptosis of LKS cells (Fig. 4A), which restored the numbers of LKS cells to levels comparable with *BCL2* littermate controls (Fig. 4B). Reduced apoptosis and increased numbers of LKS in H2K-BCL2 transgenic mice has been previously reported[20]. In addition to rescue of cell survival and cell numbers, *BCL2* over-expression restored the *in vitro* growth of myeloid and erythroid *NHD13* progenitors (Fig. 4*C*).

Apoptosis is a postulated mechanism of cytopenias in MDS although there is little direct evidence to support this hypothesis[21]. In the *NHD13* mice, blocking apoptosis corrected the macrocytic anemia of three-month old mice (Fig. 4D). Platelet numbers were not restored to wild-type levels, although they were comparable to the platelet numbers observed in the *BCL2* mice (Fig. 4D), which are known to be thrombocytopenic[12]. Thus, apoptosis was an important mechanism of cytopenia in this model.

Blocking apoptosis by enforced BCL2 expression suggested a cell intrinsic trigger of cell death[2]. However, BCL2 can inhibit extrinsic triggers of apoptosis in so-called type II cells (hepatocytes, beta-cells of the pancreas and neutrophils) by antagonizing tBID, a pro-apoptotic

BH3-only protein that is activated by caspase-8 in response to death receptor stimulation[22-25]. However, we found that BCL2 over-expression was unable to inhibit TNF-induced apoptosis of myeloid progenitor cells (Fig. S5) and given there was no demonstrable activated caspase 8 (Fig. 2*D*), it seemed unlikely that BCL2 was inhibiting apoptosis through the death receptor pathway.

**Overexpression of BCL2 prevents leukemic transformation.** Leukemic transformation of MDS is associated with higher expression of BCL2[7] and experimentally, *Bcl2* and mutant *N-ras* co-operate to generate a mouse model of MDS[26]. In other disease models, enforced expression of BCL2 accelerates Myc-induced malignancies[27-29]. To evaluate the effect of BCL2 expression in leukemic transformation of MDS, we followed cohorts of mice for 12 months. Consistent with our previous data[8], 43% of the *NHD13* mice (9 of 21) succumbed to AML by 12 months of age (Fig. 5*A*). In contrast and contrary to expectation, none of the 27 *NHD13*/*BCL2* mice developed AML within this time frame despite abnormal expression of the homeobox genes to levels greater than *NHD13* alone (Fig. 5*B*). The absence of AML in *NHD13*/*BCL2* mice was not attribution to early deaths from T-cell acute lymphoblastic leukemia (T-ALL), which developed in *NHD13* mice at a similar frequency and onset (Fig. 5*C*). Follicular-like B-cell lymphomas were the predominant cause of death in *BCL2* mice as previously described[30]. Consequently, the difference in overall survival between *NHD13*/*BCL2* and *NHD13* mice was explained by the prevention of AML (Fig. 5*D*). Thus, apoptosis is required for transformation of pre-malignant cells in this disease model.

**Blocking apoptosis restores quiescence and reduces DNA damage.** Apoptosis is required for the formation of γ-radiation-induced thymic lymphoma[31,32]. In that model, it was postulated that preventing γ-radiation-induced apoptosis by BCL2 over-expression or deficiency of the pro-

apoptotic BH3-only protein PUMA (essential for DNA damage-induced, p53-mediated apoptosis) abrogated compensatory proliferation and replication stress-associated DNA damage of BM-derived LKS cells, the cell of origin of thymic lymphoma. To determine whether a similar mechanism underpinned the prevention of AML from pre-malignant *NHD13* progenitors, we examined the cell cycle of the LKS population in *NHD13*/*BCL2* mice (Fig. 6*A*). Expression of the *BCL2* transgene alone had no significant effect on cell quiescence, but *BCL2* over-expression in *NHD13* LKS cells corrected the cell cycle defect seen in NHD13 progenitors.

To explore the cell cycle changes, we examined expression of the major cell cycle regulators: *Cdkn1a* (*p21*) and *Cdkn1b* (*p27*). The reduced quiescence of pre-malignant NHD13 progenitors correlated with reduced expression of *p21* (Fig. 6*B*) with no detectable change in *p27* (Fig. S6). Thus, the restoration of cell quiescence may be explained by increased *p21* expression in *NHD13/BCL2* pre-malignant cells.

Replicative stress induced by oncogenes leads to the formation of DNA double-strand breaks (DSBs)[5]. H2AX is a variant H2A histone protein, which becomes phosphorylated (γH2AX) when associated with DSBs, and can thereby be used as a marker of DSB occurrence. Consistent with oncogene-induced DNA damage, *NHD13* progenitor cells had increased γH2AX as measured by a flow-based assay that enabled exclusion of apoptotic cells by co-staining for activated caspase-3 (Fig. 6*C* and S7). Co-expression of the *BCL2* transgene reduced γH2AX levels to wild-type levels, although they remained higher than *BCL2* transgenic cells. Overall, these results demonstrate that BCL2 expression in pre-malignant progenitors restores cell cycle quiescence and reduces the formation of DSBs.

## Discussion

Using a transgenic model of MDS that recapitulates many of the clinical features of human disease, we show that BCL2 can block apoptosis, which improves peripheral blood counts and unexpectedly prevents disease progression. This supports and extends recent *in vitro* experiments that show retroviral expression of BCL2 rescued increased apoptosis of erythroid cells from low-risk subtypes of human MDS[33]. BCL2 can prevent TNF or FAS ligand-induced apoptosis of hepatocytes, β-cells of the pancreas and neutrophils through cleavage of BID by caspase 8[22,24,25]. However, apoptosis of myeloid and erythroid progenitors still occurred in *NHD13* mice lacking *Fasl* and *Tnf*. Furthermore, there was no detectable activated caspase 8 in NHD13 progenitors, and BCL2 did not block TNF-induced cell death. Although we cannot exclude some contribution from the extrinsic pathway, these findings suggest that BCL2 prevented apoptosis by inhibiting the BCL2-regulated pathway of apoptosis. The most likely trigger is oncogenic proliferative stress and DNA damage, as demonstrated by the reduced cell quiescence and increased γ-H2AX in *NHD13* progenitors.

Prevention of apoptosis by overexpression of BCL2 restored the red blood cell count of *NHD13* mice. *BCL2* transgenic mice have thrombocytopenia of unknown mechanism. Expression of the NHD13 transgene did not exacerbate this thrombocytopenia, indicating a relative rescue of thrombocytopenia. This provides *in vivo* evidence that apoptosis is an important contributor to the cytopenias of MDS and raises the therapeutic potential of blocking apoptosis to improve blood counts in early MDS. A major caveat of this approach would be the concern of promoting leukemic transformation, which is associated with elevated BCL2 levels[7]. However, we found that blocking apoptosis by BCL2 paradoxically prevented leukemic transformation despite increased numbers of pre-malignant progenitor cells with an 'oncogenic' gene expression profile

such as expression of Hox genes. This result contrasts with other mouse models of cancer, where overexpression of BCL2 promoted cancer progression. One speculative explanation for the disparate effects may be the different cell-of-origin of the cancers. BCL2 accelerates leukemias in *Eμ-Myc* and *MRP8-PMLRARα* transgenic mice, both models of progenitor-derived malignancies[29,34]. In contrast, the *NHD13* acute myeloid leukemias are likely derived from HSCs[35], which respond differently to DNA damage[36].

Recently, we have shown that blocking apoptosis by BCL2 (or absence of Puma) prevents the development of γ-radiation-induced thymic lymphoma[31]. In that model, preventing apoptosis reduced the compensatory proliferation of hematopoietic stem/progenitor cells bearing radiation-induced oncogenic lesions. Here, we show that preventing apoptosis of *NHD13* progenitors had a similar effect on cell cycle, with restoration of cellular quiescence. This suggests the abnormal cell cycle of *NHD13* progenitors was mediated by apoptosis rather than a direct effect of the *NHD13* oncogene (Fig. 7). Increased apoptosis may also explain the increased proliferation observed in human MDS[14]. It is not clear how apoptosis drives proliferation in the setting of oncogenic stress but one possibility is the release of mitogens such as Wnt3a and prostaglandin E2 by apoptotic cells, which is important for tissue regeneration[37]. Alternatively, BCL2 may directly slow cell cycle re-entry from $G_0$[38], although no such effect was seen in *BCL2* mice (Fig. 6*A*). Collectively, we propose that inhibition of apoptosis by BCL2 reduces replicative stress and DNA damage in pre-malignant cells, which reduces genomic instability, an important mechanism of acquiring additional genetic mutations for cancer progression (Fig. 7).

Several caveats of this work should be recognized. First, the *NHD13* translocation is a rare cause of human MDS and therefore, the results may not reflect other genetic causes of human MDS. Second, expression of the transgene generates much higher levels of *BCL2* than observed in advanced human MDS. Third, expression of the *BCL2* transgene occurs at the same

time as the initiating event and therefore increased expression of BCL2 in higher risk MDS may have a different outcome. Nevertheless, in this model of multistep oncogenesis, we show that gaining a survival advantage of pre-malignant cells may delay or prevent leukemic progression. These results raise a practical concern that inducing apoptosis by chemotherapy may be counter-productive, particularly in pre-malignant diseases such as low risk MDS. Although we have not directly addressed this possibility, a recent report has shown that radiation-induced killing can promote tumor regrowth by a caspase dependent mechanism[39]. Finally, our findings raise the possibility that inhibitors of apoptosis may be useful for improving cytopenias and delaying leukemic progression in low risk MDS.

## Acknowledgements

We thank Drs J Adams, P Bouillet and B Saunders for providing mouse strains, C Scott for providing reagents, M Guthridge, S Dworkin, and A Wei for insightful conversations, S Beeraka, S Vasudevan and J Corbin for technical assistance, S Zahra, L Ta and L Mizhiritsky for animal husbandry and C Li for flow cytometry. This work was supported by the National Health and Medical Research Council of Australia (Project Grant 628367, Program Grant 461221, NHMRC Australia Fellowship), the Cancer Council of Victoria, the Leukemia and Lymphoma Society (SCOR grant #7413), the NIH (CA43540), and operational infrastructure grants through the Australian Government IRISS and the Victorian State Government OIS. This research was supported by the Intramural Research Program of the NIH, NCI.

**Authorship Contributions**

C.I.S. and D.J.C. conceived of the project. C.I.S., S.M.J and D.J.C. designed the experiments and wrote the manuscript. C.I.S., J.S. and D.J.C. performed the experiments. J.J. performed the bioinformatics analysis. All authors discussed the interpretation of data and had intellectual input into the final manuscript.

**Conflict of Interest Disclosures**

C.I.S. and P.D.A. receive royalties from the National Institutes of Health Technology Transfer office for the invention of NUP98-HOXD13 mice. The remaining authors declare no competing financial interest.

## References


1. Tefferi, A, Vardiman, JW. Myelodysplastic syndromes. *N Engl J Med* 2009;361(19):1872-1885.
2. Youle, RJ, Strasser, A. The BCL-2 protein family: opposing activities that mediate cell death. *Nat Rev Mol Cell Biol* 2008;9(1):47-59.
3. Kerbauy, DB, Deeg, HJ. Apoptosis and antiapoptotic mechanisms in the progression of myelodysplastic syndrome. *Exp Hematol* 2007;35(11):1739-1746.
4. Barlow, JL*, et al.* A p53-dependent mechanism underlies macrocytic anemia in a mouse model of human 5q- syndrome. *Nat Med* 2010;16(1):59-66.
5. Halazonetis, TD, Gorgoulis, VG, Bartek, J. An oncogene-induced DNA damage model for cancer development. *Science* 2008;319(5868):1352-1355.
6. Hanahan, D, Weinberg, RA. Hallmarks of cancer: the next generation. *Cell* 2011;144(5):646-674.
7. Parker, JE, Mufti, GJ, Rasool, F, Mijovic, A, Devereux, S, Pagliuca, A. The role of apoptosis, proliferation, and the Bcl-2-related proteins in the myelodysplastic syndromes and acute myeloid leukemia secondary to MDS. *Blood* 2000;96(12):3932-3938.
8. Lin, YW, Slape, C, Zhang, Z, Aplan, PD. NUP98-HOXD13 transgenic mice develop a highly penetrant, severe myelodysplastic syndrome that progresses to acute leukemia. *Blood* 2005;106(1):287-295.
9. Slape, C, Liu, LY, Beachy, S, Aplan, PD. Leukemic transformation in mice expressing a NUP98-HOXD13 transgene is accompanied by spontaneous mutations in Nras, Kras, and Cbl. *Blood* 2008;112(5):2017-2019.

10. Korner, H, Riminton, DS, Strickland, DH, Lemckert, FA, Pollard, JD, Sedgwick, JD. Critical points of tumor necrosis factor action in central nervous system autoimmune inflammation defined by gene targeting. *J Exp Med* 1997;186(9):1585-1590.

11. Roths, JB, Murphy, ED, Eicher, EM. A new mutation, gld, that produces lymphoproliferation and autoimmunity in C3H/HeJ mice. *J Exp Med* 1984;159(1):1-20.

12. Ogilvy, S, Metcalf, D, Print, CG, Bath, ML, Harris, AW, Adams, JM. Constitutive Bcl-2 expression throughout the hematopoietic compartment affects multiple lineages and enhances progenitor cell survival. *Proc Natl Acad Sci U S A* 1999;96(26):14943-14948.

13. Dan, K*, et al.* Megakaryocyte, erythroid and granulocyte-macrophage colony formation in myelodysplastic syndromes. *Acta haematologica* 1993;89(3):113-118.

14. Lin, CW*, et al.* Proliferation and apoptosis in acute and chronic leukemias and myelodysplastic syndrome. *Leuk Res* 2002;26(6):551-559.

15. Deeg, HJ*, et al.* Negative regulators of hemopoiesis and stroma function in patients with myelodysplastic syndrome. *Leuk Lymphoma* 2000;37(3-4):405-414.

16. Varfolomeev, EE*, et al.* Targeted disruption of the mouse Caspase 8 gene ablates cell death induction by the TNF receptors, Fas/Apo1, and DR3 and is lethal prenatally. *Immunity* 1998;9(2):267-276.

17. Eklund, EA. The role of HOX genes in malignant myeloid disease. *Curr Opin Hematol* 2007;14(2):85-89.

18. Pellagatti, A*, et al.* Deregulated gene expression pathways in myelodysplastic syndrome hematopoietic stem cells. *Leukemia* 2010;24(4):756-764.

19. Boudard, D*, et al.* Expression and prognostic significance of Bcl-2 family proteins in myelodysplastic syndromes. *American journal of hematology* 2002;70(2):115-125.

20. Domen, J, Weissman, IL. Hematopoietic stem cells need two signals to prevent apoptosis; BCL-2 can provide one of these, Kitl/c-Kit signaling the other. *J Exp Med* 2000;192(12):1707-1718.

21. Greenberg, PL. Apoptosis and its role in the myelodysplastic syndromes: implications for disease natural history and treatment. *Leuk Res* 1998;22(12):1123-1136.

22. Croker, BA*, et al.* Fas-mediated neutrophil apoptosis is accelerated by Bid, Bak, and Bax and inhibited by Bcl-2 and Mcl-1. *Proc Natl Acad Sci U S A* 2011;108(32):13135-13140.

23. Jost, PJ*, et al.* XIAP discriminates between type I and type II FAS-induced apoptosis. *Nature* 2009;460(7258):1035-1039.

24. Kaufmann, T*, et al.* Fatal hepatitis mediated by tumor necrosis factor TNFalpha requires caspase-8 and involves the BH3-only proteins Bid and Bim. *Immunity* 2009;30(1):56-66.

25. McKenzie, MD*, et al.* Proapoptotic BH3-only protein Bid is essential for death receptor-induced apoptosis of pancreatic beta-cells. *Diabetes* 2008;57(5):1284-1292.

26. Omidvar, N*, et al.* BCL-2 and mutant NRAS interact physically and functionally in a mouse model of progressive myelodysplasia. *Cancer Res* 2007;67(24):11657-11667.

27. Jager, R, Herzer, U, Schenkel, J, Weiher, H. Overexpression of Bcl-2 inhibits alveolar cell apoptosis during involution and accelerates c-myc-induced tumorigenesis of the mammary gland in transgenic mice. *Oncogene* 1997;15(15):1787-1795.

28. Pelengaris, S, Khan, M, Evan, GI. Suppression of Myc-induced apoptosis in beta cells exposes multiple oncogenic properties of Myc and triggers carcinogenic progression. *Cell* 2002;109(3):321-334.

29. Strasser, A, Harris, AW, Bath, ML, Cory, S. Novel primitive lymphoid tumours induced in transgenic mice by cooperation between myc and bcl-2. *Nature* 1990;348(6299):331-333.

30. Egle, A, Harris, AW, Bath, ML, O'Reilly, L, Cory, S. VavP-Bcl2 transgenic mice develop follicular lymphoma preceded by germinal center hyperplasia. *Blood* 2004;103(6):2276-2283.

31. Michalak, EM*, et al.* Apoptosis-promoted tumorigenesis: gamma-irradiation-induced thymic lymphomagenesis requires Puma-driven leukocyte death. *Genes Dev* 2010;24(15):1608-1613.

32. Labi, V*, et al.* Apoptosis of leukocytes triggered by acute DNA damage promotes lymphoma formation. *Genes Dev* 2010;24(15):1602-1607.

33. Gyan, E*, et al.* Spontaneous and Fas-induced apoptosis of low-grade MDS erythroid precursors involves the endoplasmic reticulum. *Leukemia* 2008;22(10):1864-1873.

34. Kogan, SC*, et al.* BCL-2 cooperates with promyelocytic leukemia retinoic acid receptor alpha chimeric protein (PMLRARalpha) to block neutrophil differentiation and initiate acute leukemia. *J Exp Med* 2001;193(4):531-543.

35. Chung, YJ, Choi, CW, Slape, C, Fry, T, Aplan, PD. Transplantation of a myelodysplastic syndrome by a long-term repopulating hematopoietic cell. *Proc Natl Acad Sci U S A* 2008;105(37):14088-14093.

36. Seita, J, Rossi, DJ, Weissman, IL. Differential DNA damage response in stem and progenitor cells. *Cell Stem Cell* 2010;7(2):145-147.

37. Fuchs, Y, Steller, H. Programmed cell death in animal development and disease. *Cell* 2011;147(4):742-758.

38. O'Reilly, LA, Huang, DC, Strasser, A. The cell death inhibitor Bcl-2 and its homologues influence control of cell cycle entry. *Embo J* 1996;15(24):6979-6990.

39. Huang, Q*, et al.* Caspase 3-mediated stimulation of tumor cell repopulation during cancer radiotherapy. *Nat Med* 2011;17(7):860-866.

## Figure Legends

**Fig. 1.** Increased apoptosis in BM from three-month old *NHD13* mice. (A) Hematocrit (HCT), red cell mean cell volume (MCV) and platelet and neutrophil counts of three-month old *NHD13* mice (n=5) and wild-type (WT) littermate controls (n=5) (B) Proportions of Annexin-V positive and cleaved (i.e. active) caspase-3 positive LKS cells from WT and *NHD13* mice assessed by FACS (n = 3 of each genotype) (C) Representative FACS plots from cell cycle analysis of WT and NHD13 LKS cells and collated data showing cell cycle distribution ($G_0$, $G_1$ and combined $S/G_2/M$) in WT (n = 6) and *NHD13* (n=4) * indicates $G_0$ $p<0.05$ difference from WT (D) Representative FACS plots and proportions of FLK2+ LKS (n = 3 per genotype). (E) Numbers of granulocyte and macrophage colonies (CFU-GM), blast-forming units-erythroid (BFU-E) and megakaryocytic colonies (Meg-CFC) in BM from WT and *NHD13* mice (n = 3 per genotype). (F) Giemsa stain of granulocytes colonies grown in semi-solid agar demonstrating apoptotic bodies (arrows) in *NHD13* granulocyte colonies. Error bars throughout represent the SEM. * indicates $p<0.05$; ** indicates $p<0.01$; *** indicates $p < 0.001$.

**Fig. 2.** The apoptosis in NHD13 progenitors is not mediated by the death receptor pathway. (A) Proportions of Annexin-V positive LKS cells assessed by FACS (n = 3 of each geneotype). (B) CFU-GM and (C) BFU-E numbers in wild type and NHD13 BM on wild type, $FasL^{gld/gld}$ or $TNF^{-/-}$ backgrounds (n = 3 of each genotype). (D) Western blot showing the presence of native and cleaved (active) caspase 8 in wild type LK cells, NHD13 LK cells, wild type thymocytes treated with or without FasL. Actin is shown as a loading control. All experiments performed using three-month old mice. Error bars represent the s.e.m. * indicates $p < 0.05$. *** indicates $p < 0.001$.

**Fig 3.** Bcl2 expression is reduced in NHD13 LK cells. (A) Quantification of Bcl2 levels by Q-RT-PCR in LK cells from wild-type (WT) and NHD13 mice (n = 3 of each genotype, each sample is a pool of three mice) and marrow cells from NHD13 mice which developed AML (n = 5). ** indicates $p < 0.01$. (B) Representative histograms of Bcl2 protein in wild-type (WT) and *NHD13* LK cells measured by FACS. The dashed lines represent the isotype controls. The mean cell fluorescence of Bcl2 protein in *NHD13* LK cells relative to WT LK cells was calculated from three-month old mice (n=3 of each genotype).

**Fig. 4.** Enforced *BCL2* expression inhibits the excess apoptosis of *NHD13* hematopoietic progenitors. (A) Proportions of Annexin-V positive LKS cells from WT, *NHD13*, *BCL2* and *NHD13/BCL2* mice (n = 3 of each genotype). (B) Proportions of LKS cells in BM from three mice of each genotype. (C) CFU-GM and BFU-E numbers in BM from three mice of each genotype. (D) Hematocrit (HCT), red cell mean cell volume (MCV) and platelet count of five mice of each genotype. All measurements were made on three-month old mice. Error bars represent the SEM. NS indicates $p>0.05$; * indicates $p<0.05$; ** indicates $p<0.01$; *** indicates $p<0.001$.

**Fig. 5.** *BCL2* prevents transformation of MDS to AML in *NHD13* mice. (A) Kaplan-Meier AML-free survival of WT (n=20), *NHD13* (n=34), *BCL2* (n=23) and*NHD13*/*BCL2* (n=29) mice. Mice that died from causes other than AML were censored at time of death. Note that WT, *BCL2* and *NHD13*/*BCL2* lines are overlaid (indicated by A). (B) Q-RT-PCR analysis of HoxA9, HoxB7, HoxC6 and Pbx3 expression in LK cells of each indicated genotype (n=3 of each genotype). (C) T-ALL-free survival in the same cohorts of mice. Mice that died from causes other than T-ALL

were censored at time of death. Note that the WT and *BCL2* lines are overlaid (indicated by A). (D) Overall survival of the same cohorts of mice. p-values indicate difference from the survival of *NHD13* mice. (D) Q-RT-PCR analysis of HoxC6, HoxB7, HoxA9 and Pbx3 expression in LK cells from three mice of each genotype. * indicates $p<0.05$. ** indicates $p<0.01$. *** indicates $p<0.001$.

**Fig. 6.** BCL2 restores cell cycle quiescence and limits DNA damage in NHD13 progenitors. (A) Cell cycle distribution ($G_0$, $G_1$ and combined S/$G_2$/M) of LKS cells from WT (n = 6), *NHD13* (n=4), *BCL2* (n = 5), and *NHD13*/*BCL2* (n = 5) mice. * indicates $G_0$ $p<0.05$ difference from WT. (B) *Cdkn1a* mRNA expression in LK cells from three mice of each genotype. (C) FACS quantification of gH2AX levels in non-apoptotic (caspase-3 negative) LK cells from three mice of each genotype. NS indicates $p>0.05$. * indicates $p<0.05$.

**Fig.7.** Model of how apoptosis can promote malignant transformation of pre-malignant cells. Pre-malignant cells harboring a single oncogenic lesion undergo apoptosis triggered by oncogenic stress. Apoptosis promotes proliferative stress and DNA damage through unknown mechanisms, which leads to genomic instability and accumulation of additional genetic events necessary for progression to an aggressive malignancy.

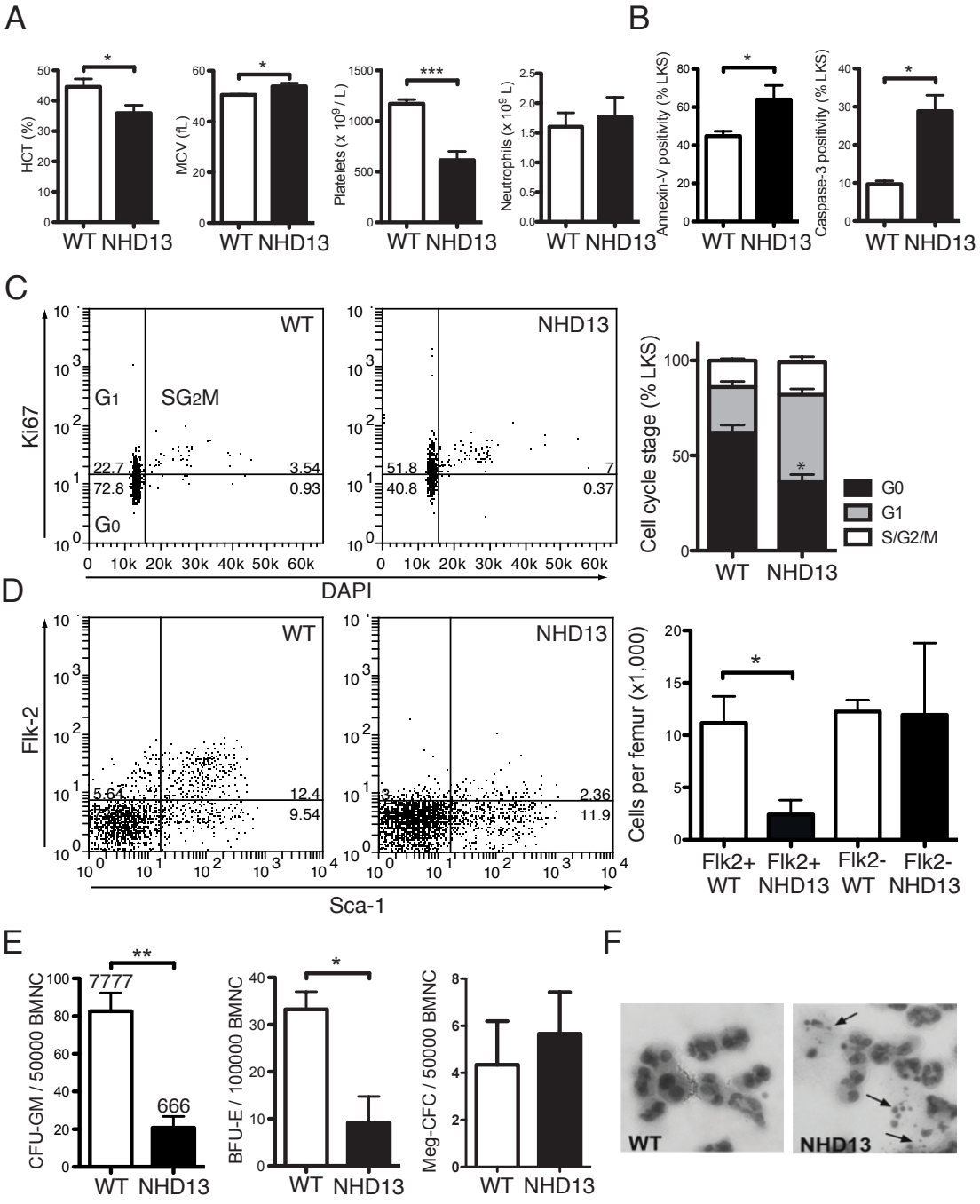
A
B
C
D
E
F
HCT (%)
MCV (fL)
Platelets (x 10^9 / L)
Neutrophils (x 10^9 L)
Annexin-V positivity (% LKS)
Caspase-3 positivity (% LKS)
WT NHD13
Ki67
DAPI
G1
SG2M
G0
22.7
72.8
3.54
0.93
51.8
40.8
7
0.37
Cell cycle stage (% LKS)
G0
G1
S/G2/M
Flk-2
Sca-1
5.64
12.4
9.54
2.36
11.9
Cells per femur (x1,000)
Flk2+ WT
Flk2+ NHD13
Flk2- WT
Flk2- NHD13
CFU-GM / 50000 BMNC
7777
666
BFU-E / 100000 BMNC
Meg-CFC / 50000 BMNC
WT
NHD13

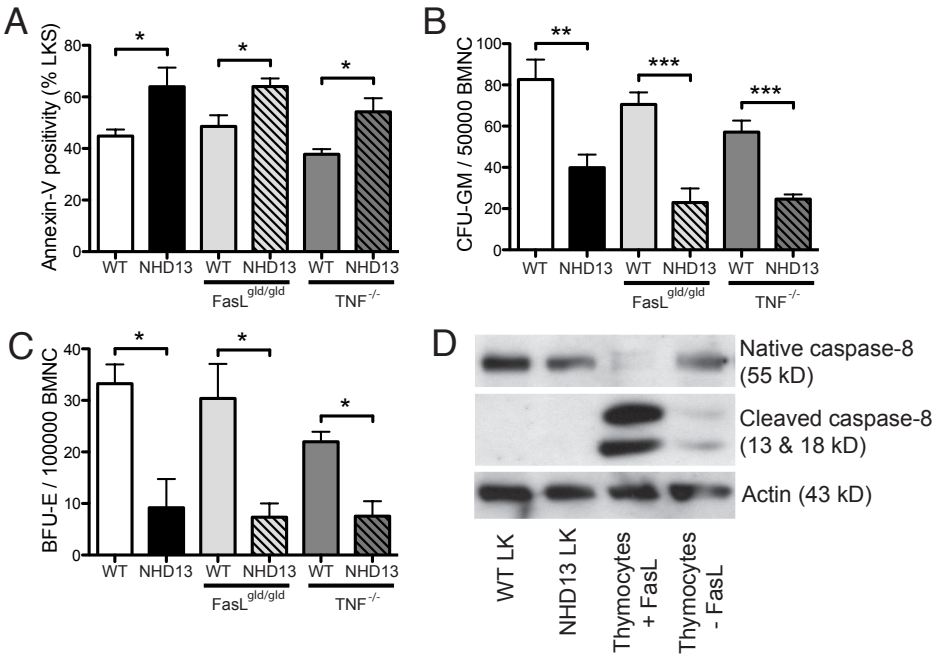
A
Annexin-V positivity (% LKS)
0
20
40
60
80
*
*
*
WT
NHD13
WT
NHD13
WT
NHD13
FasL gld/gld
TNF -/-
B
CFU-GM / 50000 BMNC
0
20
40
60
80
100
**
***
***
WT
NHD13
WT
NHD13
WT
NHD13
FasL gld/gld
TNF -/-
C
BFU-E / 100000 BMNC
0
10
20
30
40
*
*
*
WT
NHD13
WT
NHD13
WT
NHD13
FasL gld/gld
TNF -/-
D
Native caspase-8
(55 kD)
Cleaved caspase-8
(13 & 18 kD)
Actin (43 kD)
WT LK
NHD13 LK
Thymocytes
+ FasL
Thymocytes
- FasL

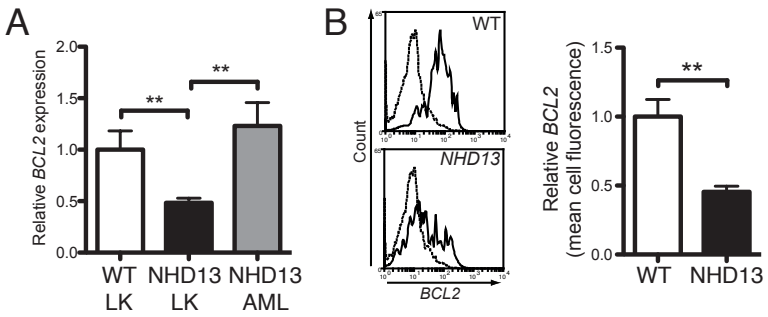
A
Relative BCL2 expression
2.0
1.5
1.0
0.5
0.0
**
**
WT LK
NHD13 LK
NHD13 AML
B
Count
WT
NHD13
BCL2
Relative BCL2 (mean cell fluorescence)
1.5
1.0
0.5
0.0
**
WT
NHD13

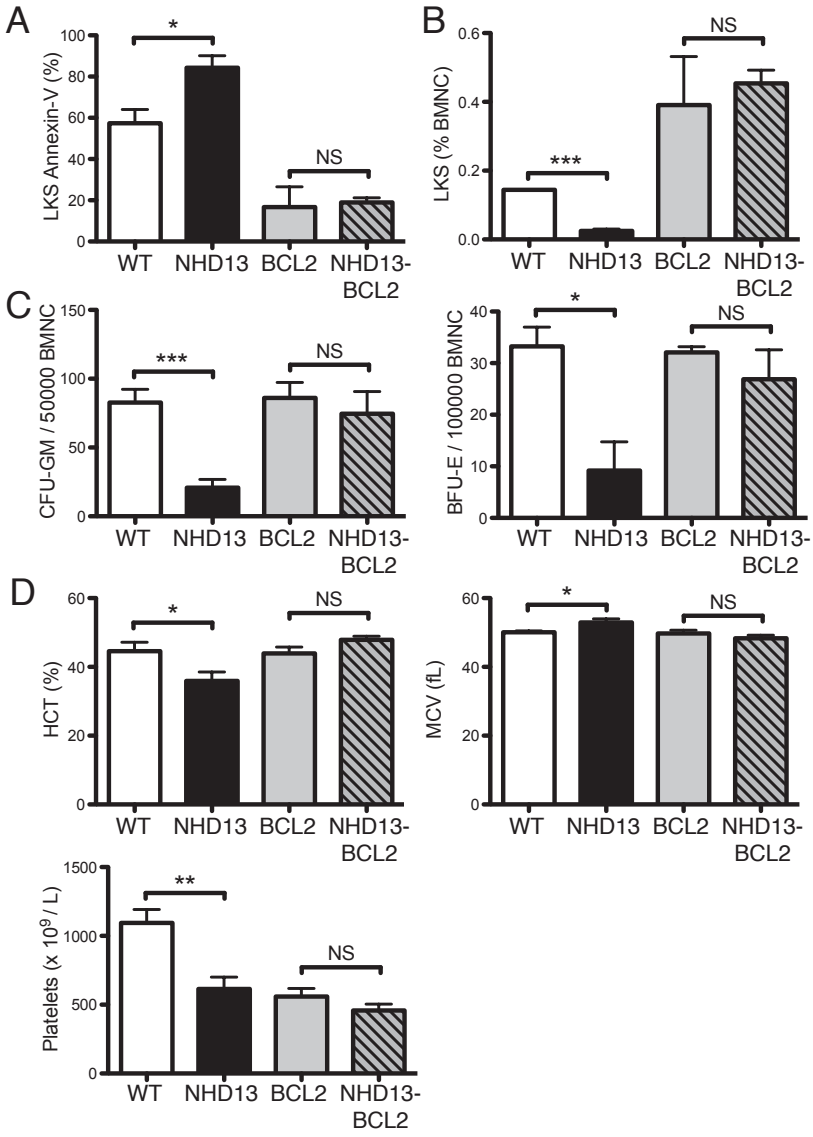
A
LKS Annexin-V (%)
100
80
60
40
20
0
*
NS
WT
NHD13
BCL2
NHD13-BCL2
B
LKS (% BMNC)
0.6
0.4
0.2
0.0
***
NS
WT
NHD13
BCL2
NHD13-BCL2
C
CFU-GM / 50000 BMNC
150
100
50
0
***
NS
WT
NHD13
BCL2
NHD13-BCL2
BFU-E / 100000 BMNC
40
30
20
10
0
*
NS
WT
NHD13
BCL2
NHD13-BCL2
D
HCT (%)
60
40
20
0
*
NS
WT
NHD13
BCL2
NHD13-BCL2
MCV (fL)
60
40
20
0
*
NS
WT
NHD13
BCL2
NHD13-BCL2
Platelets (x 10^9 / L)
1500
1000
500
0
**
NS
WT
NHD13
BCL2
NHD13-BCL2

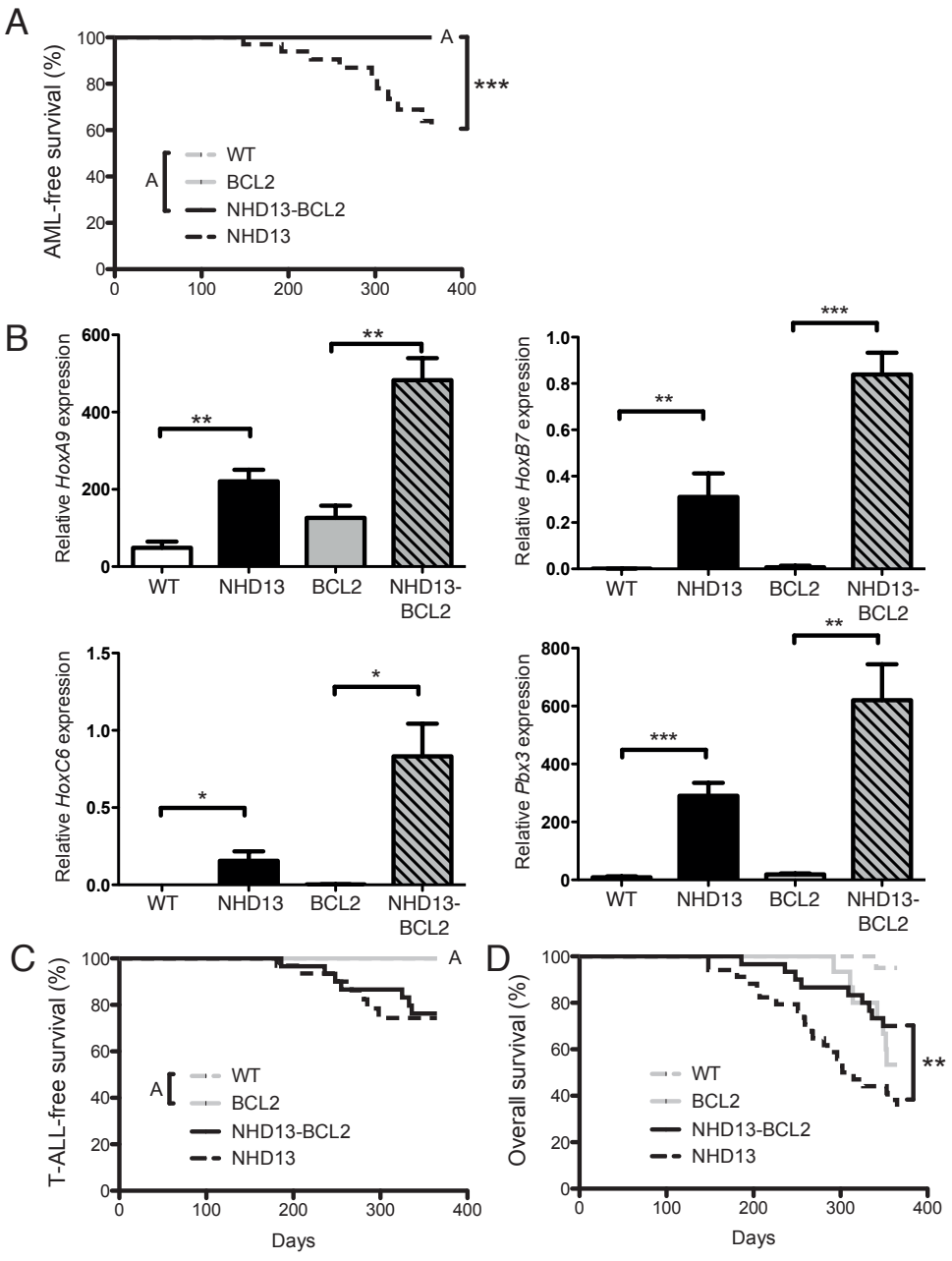
A
AML-free survival (%)
100
80
60
40
20
0
0
100
200
300
400
A
***
A
WT
BCL2
NHD13-BCL2
NHD13
B
Relative HoxA9 expression
600
400
200
0
**
**
WT
NHD13
BCL2
NHD13-BCL2
Relative HoxB7 expression
1.0
0.8
0.6
0.4
0.2
0.0
**
***
WT
NHD13
BCL2
NHD13-BCL2
Relative HoxC6 expression
1.5
1.0
0.5
0.0
*
*
WT
NHD13
BCL2
NHD13-BCL2
Relative Pbx3 expression
800
600
400
200
0
***
**
WT
NHD13
BCL2
NHD13-BCL2
C
T-ALL-free survival (%)
100
80
60
40
20
0
0
100
200
300
400
Days
A
A
WT
BCL2
NHD13-BCL2
NHD13
D
Overall survival (%)
100
80
60
40
20
0
0
100
200
300
400
Days
**
WT
BCL2
NHD13-BCL2
NHD13

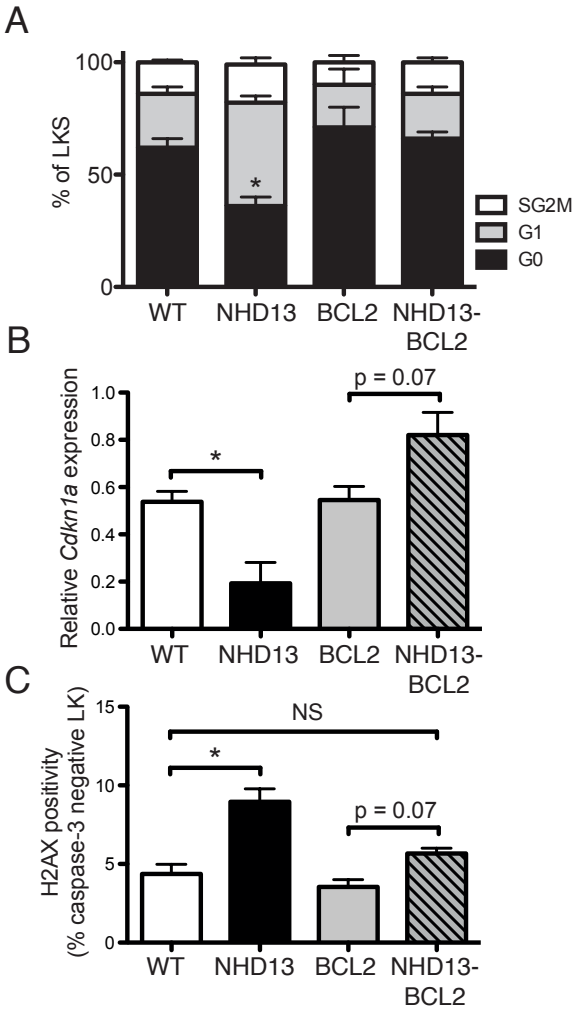
A
100
50
0
% of LKS
*
SG2M
G1
G0
WT
NHD13
BCL2
NHD13-BCL2
B
Relative Cdkn1a expression
1.0
0.8
0.6
0.4
0.2
0.0
p = 0.07
*
WT
NHD13
BCL2
NHD13-BCL2
C
H2AX positivity (% caspase-3 negative LK)
15
10
5
0
NS
*
p = 0.07
WT
NHD13
BCL2
NHD13-BCL2

Slape_Fig7

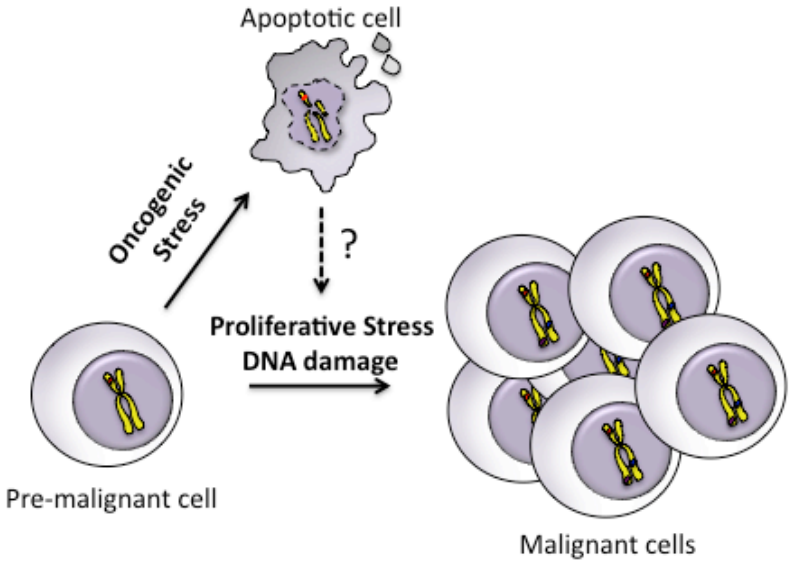
Apoptotic cell
Oncogenic Stress
?
Proliferative Stress
DNA damage
Pre-malignant cell
Malignant cells

Supplemental Figure 1

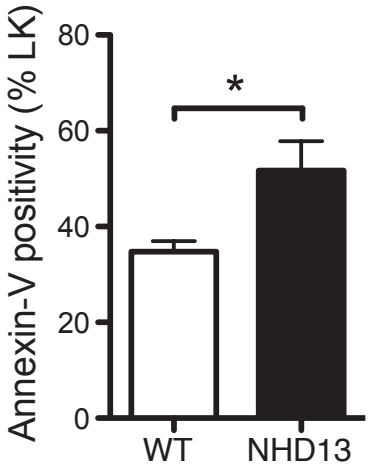


Figure S1. Detection of Annexin-V in LK cells. Proportions of Annexin-V positive and LK cells from WT and NHD13 mice assessed by FACS (n = 3 of each genotype). * indicates $p<0.05$.

Supplemental Figure 2

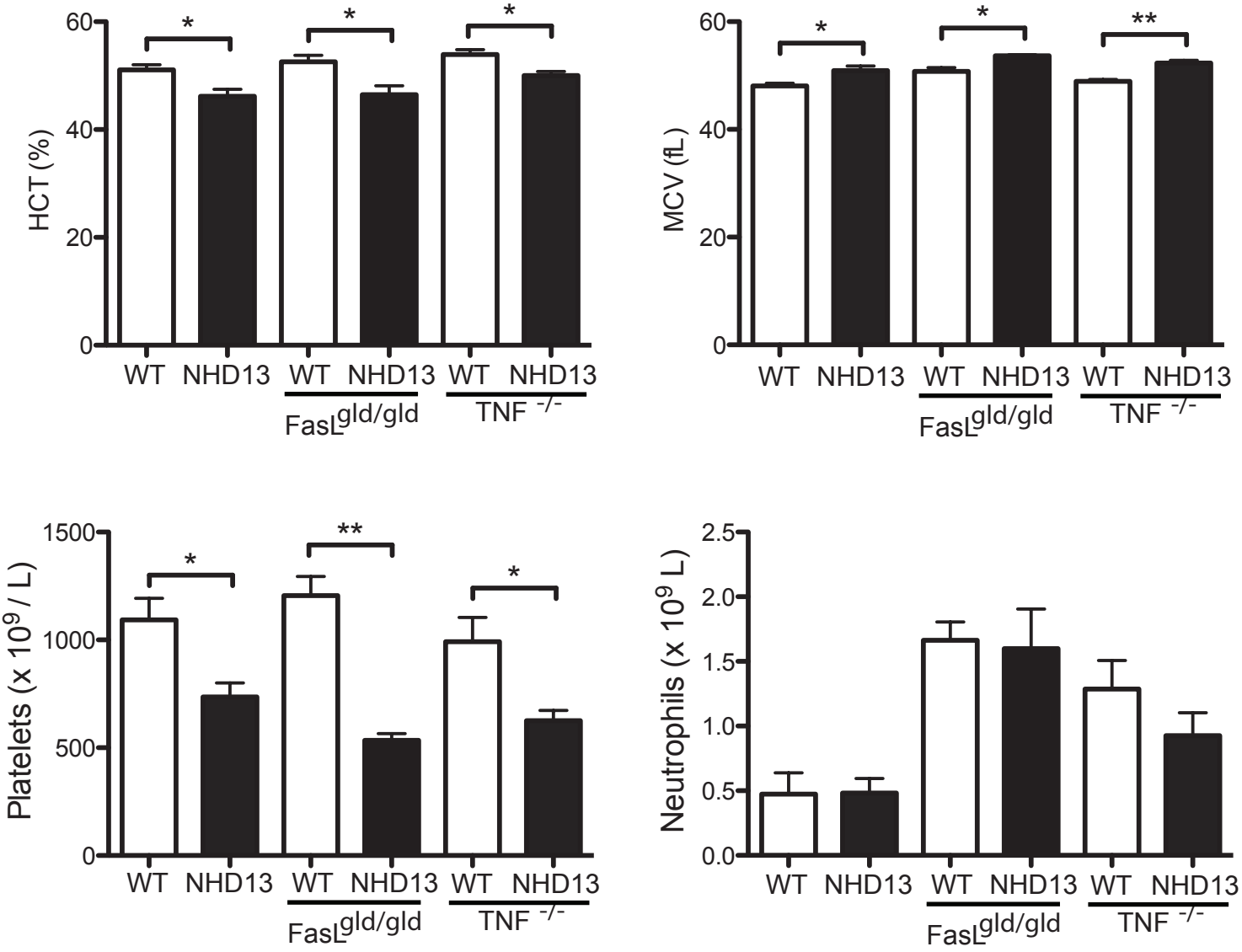


Figure S2. Peripheral blood counts are not rescued by deficiencies in death receptor ligands. Hematocrit (HCT), red cell mean cell volume (MCV) and platelet and neutrophil counts of three-month old NHD13 mice (n=5) and wild-type (WT) littermate controls on wild type, $FasL^{gld/gld}$ or $TNF^{-/-}$ backgrounds (n = 3 of each genotype). * indicates $p<0.05$. ** indicates $p<0.01$.

# Supplemental Figure 3

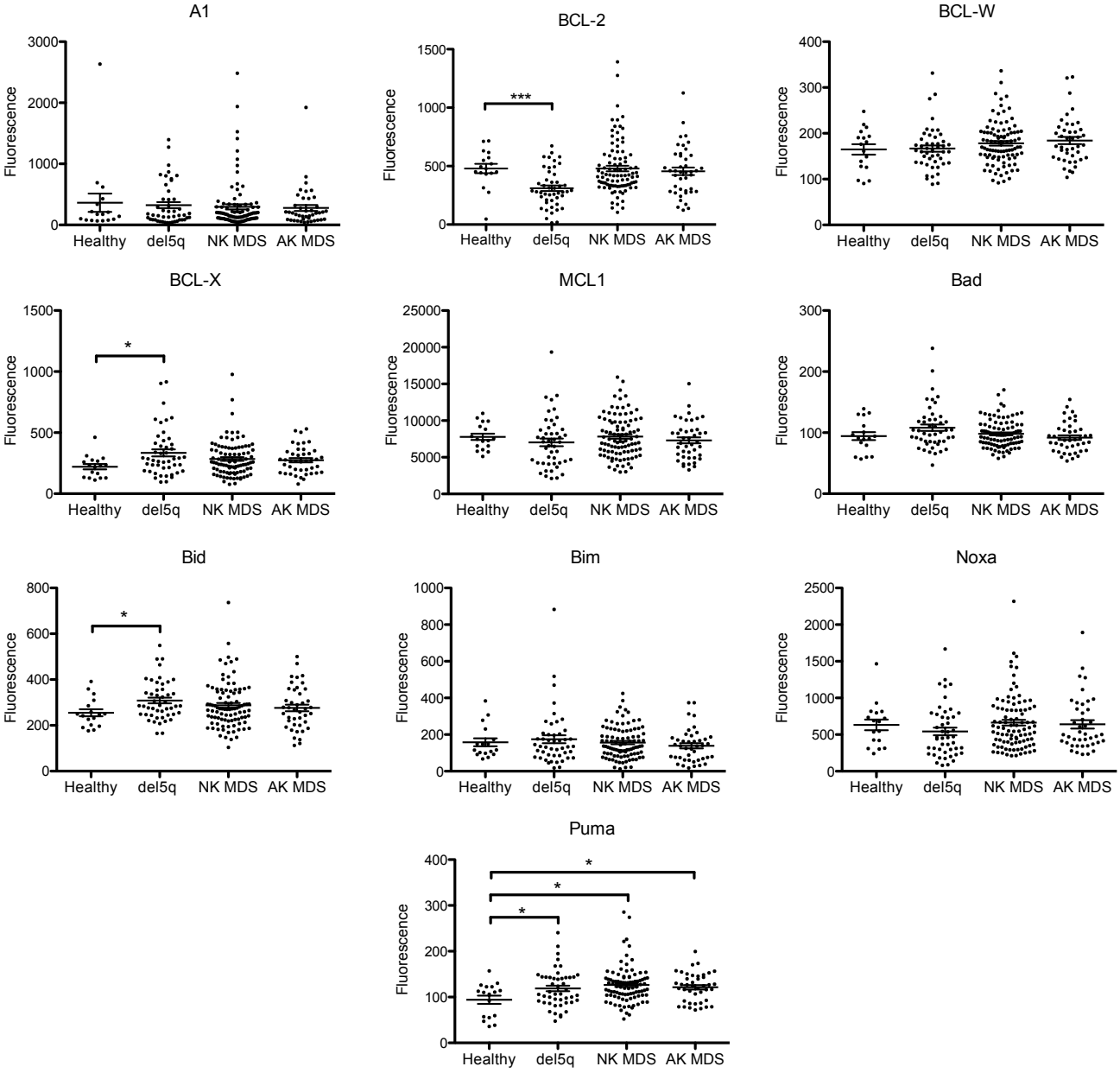


Figure S3. mRNA expression of various *BCL2* family genes in CD34+ cells isolated from healthy controls (n=17), MDS with del 5q (n = 47), MDS with normal karyotype (NK, n = 94) and MDS with abnormal karyotype (AK) other than del5q (n = 42). * indicates $p < 0.05$. *** indicates $p < 0.001$

Supplemental Figure 4

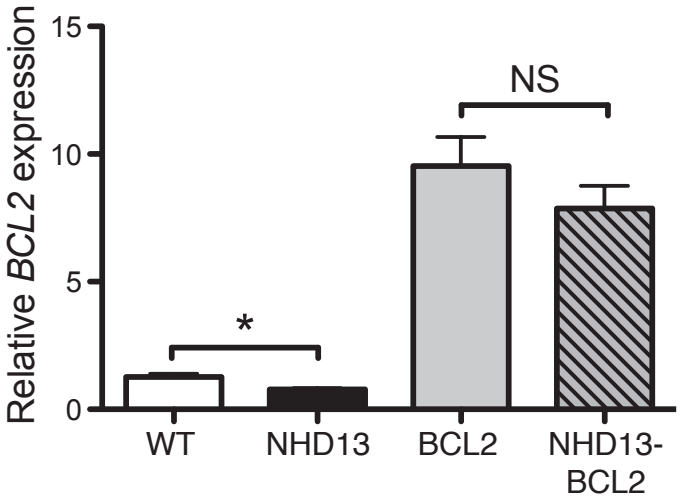


Figure S4. Q-RT-PCR quantification of BCL-2 mRNA levels in LK cells from wild-type (WT), NHD13, vav-BCL-2 and NHD13/vav-BCL-2 mice (n = 3 of each genotype). * indicates $p<0.05$.

Supplemental Figure 5

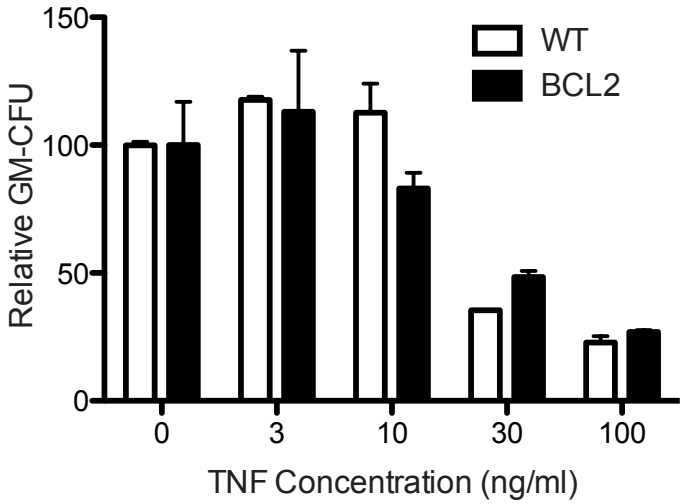


Figure S5. Granulocyte-macrophage colonies (GM-CFU) grown from WT or vav-BCL-2 bone marrow cultured in increasing concentrations of tumor necrosis factor (TNF) (n = 3 of each genotype). NS indicates $p>0.05$. * indicates $p<0.05$.

Supplemental Figure 6

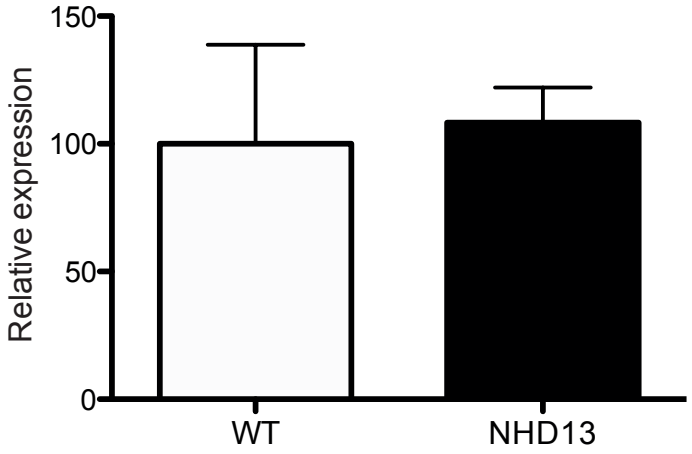


Figure S6. Q-RT-PCR quantification of p27 (CDKN1B) mRNA levels in LK cells from wild-type (WT), NHD13 mice (n = 3 of each genotype). No significant difference is evident.

Supplemental Figure 7

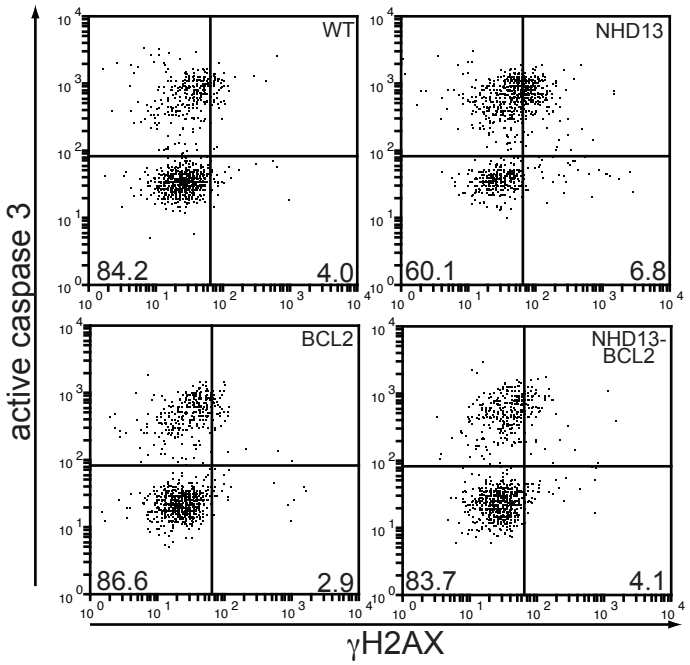


Figure S7. Detection of γH2AX in non-apoptotic cells. Cleaved (active) caspase-3 was used to discriminate apoptotic cells (in the upper two quadrants of each plot), and the non-apoptotic cells were used to calculate the percentage of cells positive for active γH2AX (lower right quadrant). One representative sample is shown from each genotype (denoted in upper-right corner of each plot).

**Table S1**

| Gene | Fold Change Increased | Gene | Fold Change Reduced |
|---|---|---|---|
| Hoxc6 | 440 | Fkbp9 | 153 |
| Hoxb7 | 233 | Igkv14-126 | 45.3 |
| Zfpm2 | 82.2 | Gspt2 | 37.3 |
| Pbx3 | 30.0 | Serpinf1 | 11.2 |
| Hoxb5 | 25.4 | Tceal8 | 8.92 |
| Hoxa5 | 6.36 | Tnfsf12-tnfsf13 | 7.46 |
| Ttc39a | 4.95 | Ryk | 6.70 |
| Hoxa9 | 4.48 | Ppic | 6.61 |
| Hoxa7 | 3.96 | Bex4 | 6.39 |
| Arhgdig | 3.54 | Snn | 6.06 |
| Oasl1 | 3.17 | Snca | 5.99 |
| P2ry1 | 3.13 | Tsp50 | 5.89 |
| Hopx | 3.11 | Gdf3 | 5.80 |
| Xlr4a | 2.95 | Epb4.1l4b | 5.53 |
| Pex11a | 2.90 | Smo | 5.20 |
| Oasl1 | 2.67 | Lzts2 | 4.48 |
| Agrn | 2.27 | Ifitm1 | 4.25 |
| Ascc3 | 2.14 | Fam110b | 3.74 |
| Mars2 | 2.02 | Nav1 | 3.70 |
| Insl6 | 2.01 | Bcl2 | 3.61 |
| | | Rbpms | 3.56 |
| | | Ndrl | 3.48 |
| | | Meis1 | 3.36 |
| | | Csrp3 | 3.32 |
| | | Akr1c12 | 3.30 |
| | | Dpp4 | 2.90 |
| | | Fnbp1l | 2.87 |
| | | P2ry14 | 2.80 |
| | | Il11ra1 | 2.78 |
| | | Ndrg1 | 2.64 |
| | | Gcnt2 | 2.61 |
| | | Myh10 | 2.54 |
| | | Il12a | 2.43 |
| | | Rhobtb3 | 2.41 |
| | | Rgs1 | 2.20 |
| | | Rnf125 | 2.19 |
| | | Fkbp11 | 2.18 |
| | | Pde4b | 2.18 |
| | | Fam69b | 2.17 |
| | | Slco3a1 | 2.12 |
| | | Egr1 | 2.11 |
| | | Tmem176a | 2.10 |
| | | C85492 | 2.09 |
| | | Gpr171 | 2.06 |
| | | Fam134b | 2.05 |